Measurement Methods for Nanoparticles in Indoor and Outdoor Air

Christof Asbach, Simon Clavaguera, and Ana Maria Todea

Abstract A large variety of measurement methods for the characterization of airborne nanoparticles in indoor or outdoor air exist. The choice of an appropriate method depends strongly on the questions to be tackled. If the aerosol is to be characterized only for a single location, one may use stationary equipment that is rather bulky but provides the most details and is most accurate. Spatially resolved measurements can only be conducted with portable or personal measurement equipment which provide a limited dataset with lower accuracy. Furthermore, the metrics to be measured (e.g., number, surface area of mass concentration, chemical composition, etc.) determine the choice of measurement methods as no single method can do it all. Another determining factor is the time resolution of the instruments. While direct-reading monitors deliver the information with high time resolution (often 1 s) and hence allow for linking the measured concentration to certain activities, samplers collect the particles for subsequent analyses and therefore provide an average over the sampling time. Consequently, the choice of a measurement instrument for the characterization of airborne nanoparticles remains a compromise. In many practical applications, the combination of different techniques may be required.

Keywords Indoor Air, Outdoor Air, Air Quality, Nanoparticles, Exposure, Aerosol Measurement

C. Asbach (✉) and A.M. Todea
Institut für Energie- und Umwelttechnik e. V. (IUTA), Air Quality and Filtration Unit, Bliersheimer Straße 58-60, 47229 Duisburg, Germany
e-mail: asbach@iuta.de

S. Clavaguera
NanoSafety Platform, Commissariat à l'Energie Atomique et aux Energies Alternatives (CEA), Univ. Grenoble Alpes, Grenoble 38054, France

M. Viana (ed.), *Indoor and Outdoor Nanoparticles: Determinants of Release and Exposure Scenarios*, Hdb Env Chem (2016) 48: 19–50, DOI 10.1007/698_2015_423,

Contents

1 Introduction

Nanoparticles are ubiquitous in indoor and outdoor air. They can stem from a large variety of sources. According to the definition of the European Commission, a nanomaterial is "a natural, incidental or manufactured material containing particles, in an unbound state or as an aggregate or as an agglomerate and where, for 50 % or more of the particles in the number size distribution, one or more external dimensions is in the size range 1–100 nm" [1]. Nanomaterials can hence be intentionally produced synthetic particles which are used in numerous applications such as cosmetics, coatings, or tires; they can be by-products from human activities, e.g., soot from incomplete combustion; or they can be naturally produced particles, e.g., sea salt from ocean mist or nucleation particles. Although it may not be strictly correct, the term nanoparticle is used synonymously with nanomaterial according to the EC definition here. In the past, several studies have shown that nanoparticles may cause more severe biological effects than the same mass dose of larger particles of identical chemical entity [2–4]. The assessment of exposure to airborne nanoparticles in both indoor and outdoor environments has therefore raised increased attention in the recent years. The traditional exposure assessment focused on wider size fractions, e.g., all particles below 10 µm (PM_{10}) or 2.5 µm ($PM_{2.5}$) in ambient measurements or below 4 µm (respirable fraction) in workplace exposure assessment. These measurements determine the total mass concentration of the respective particle size fraction. The mass concentration scales with the third power of the particle diameter and therefore weights larger particles much more strongly than smaller ones. As an example, a single 10 µm particle has the same mass as one thousand 1 µm particles, one million 100 nm particles, or one billion 10 nm particles. Although nanoparticles typically occur in much higher numbers than micron-sized particles, it is obvious that they usually only contribute a very small fraction to the total mass concentration. To obtain a better representation of the presence of nanoparticles, metrics other than the mass concentration are therefore required. An example for a bimodal particle size distribution is shown in Fig. 1. The graph shows the same size distribution, represented as number size distribution, surface area size distribution, and mass size distribution. Both modes of the distribution are lognormal. The first mode has a count median diameter (CMD) of 100 nm, a geometric standard deviation (σ_g) of 1.7, and a total number concentration of 500,000 1/cm^3, and the second mode has a CMD of 3,000 nm, a σ_g of 2.0,

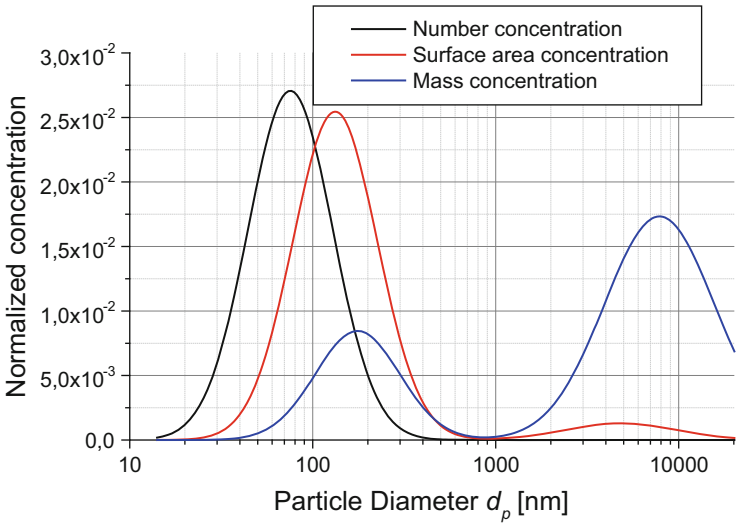

Fig. 1 Example for a bimodal particle size distribution; first mode with a CMD at 100 nm and 500,000 1/cm^3 and second mode with CMD at 3,000 nm (3 µm) and 1,000 1/cm^3, represented as number size distribution (*black*), surface area size distribution (*red*), and mass size distribution (*blue*); for clearer representation, all data have been normalized with respect to the total concentration

and a total number concentration of 1,000 1/cm^3. For better representation, the graphs have been normalized to the respective total concentration. The figure shows that in the number size distribution the second mode is invisible, due to its low number concentration, whereas it contributes the major part to the mass size distribution. In the surface area size distribution, the first mode is still dominant, but the second mode is clearly visible. The surface area concentration has raised increased attention in the recent years, because several studies indicated that the biological effects seem to correlate best with the total particle surface area dose [3, 5]. Currently, no instrument exists that is capable of measuring the particle surface area concentration of airborne particles. The only surface area-related metric that can be measured is the lung-deposited surface area (LDSA) concentration, i.e., the fraction of the total airborne surface area concentration that upon inhalation would be retained in the human lung.

Besides the particle size, the particle morphology and chemical composition can also play a significant role in the toxicity of inhaled particles. It was, for example, shown that the effects of CeO_2 particles were significantly higher than that of TiO_2 particles for the same mass dose and similar particle sizes. On the contrary, $BaSO_4$ particles produced no noticeable effects [6]. Poland et al. [7] found that carbon nanotubes (CNTs) can have asbestos-like effects, but only if they are stiff and have a high aspect ratio and occur as a single CNT and not in bundles.

The available instrumentation to assess exposure to nanoparticles can be differentiated into stationary, portable, and personal equipment. Furthermore, it can be

differentiated into (quasi-)real-time instruments that deliver the results with high time resolution and particle samplers that collect particles for subsequent chemical and/or morphological analyses.

Stationary equipment is typically the most accurate but only gives information for a single measurement location. In workplace exposure assessment, stationary equipment is mainly used for tier 3 measurements. The instruments are mains powered and bulky so that the transport to another location requires quite some effort. Portable instruments are much smaller and battery operated so that they can easily be moved from one location to another, i.e., they are most suitable for tier 2 measurements in workplace exposure assessment. Their accuracy and sizing resolution (if applicable) are typically lower than for stationary instruments. Personal instruments are small enough to be carried by a person and measure/sample in the breathing zone, i.e., within a 30 cm hemisphere around the mouth and nose of the individual [8] in order to measure the true personal exposure. The choice of an instrument or a suite of instruments always remains a compromise between the size of the instrument(s) on the one side and the wealth and quality of the data on the other side. If the intention is to obtain a best possible characterization of the aerosol, then a large set of equipment is required that is immobile and expensive but provides the most detailed analysis with high accuracy. In contrast, if the intention is to keep track of the exposure of an individual, then only small, person-carried instruments come into play, which however only deliver a limited dataset with lower accuracy.

The intention of this book chapter is to provide an overview of the existing measurement methods for nanoparticles, their typical field of application, as well as their strengths and weaknesses.

2 Measurement Methods

This section provides the details on the measurement methods and instruments used for the quantification of airborne nanoparticles. The description starts with the stationary equipment which comprises the most accurate instruments. Portable and personal instruments were developed later than the stationary instruments and use the same or similar techniques. The instrument groups are further differentiated into time-resolving (real-time) instruments and time-integrating (sampling) instruments. While the time-resolving instruments all use measurement methods specific for a certain metric, time-integrating instruments sample particles on substrates which can be analyzed for different purposes, e.g., morphology or chemical composition.

2.1 Stationary Equipment

Stationary equipment is characterized by the instrument size, which is typically bulky, and its need for mains power, which immobilizes the equipment. The equipment is furthermore differentiated into time resolving and time integrating. Time-resolving instruments are those that deliver the results in (quasi-)real time with high time resolution, whereas time-integrating instruments sample the particles onto substrates or filters for subsequent analyses of the chemical composition or the particle morphology. The time-integrated results can be either qualitative (e.g., proof for the presence or absence of a certain particle morphology like CNTs) or quantitative as an average of the sampling time. Stationary equipment is typically most accurate and provides the highest size resolution (if applicable) and therefore used for detailed aerosol analyses like in tier 3 workplace exposure assessment.

2.1.1 Time-Resolving Instruments

Measurement of Particle Number Concentration

Only particles larger than approximately half the wavelength of light can be detected optically. Conventional optical particle counters therefore only detect particles down to approximately 250 nm and are not further covered here. Condensation particle counters (CPCs) artificially enlarge the particles to make them optically detectable. As shown in Fig. 2, the incoming aerosol is first guided through a heated saturator, in which a working fluid (usually butanol, isopropyl alcohol, or water) is evaporated until the air is saturated with vapor. Typical sampling flow rates are between 0.3 and 1.5 L/min. In the following condenser, the temperature is reduced, resulting in a supersaturation of the working fluid vapor. The particles now act as condensation nuclei, i.e., vapor condenses onto the particle surfaces and the aerosol leaving the condenser contains only droplets with the original particles inside. Since the vapor is homogenously distributed onto all particles, each droplet represents exactly one particle so that counting of the droplets in the downstream optical sensor also yields the number (concentration) of the particles in the incoming aerosol. Growth factors between the original particle diameter and the eventual droplet diameter between 100 and 1,000 are common [9]. The eventual droplet size distribution is, however, quite narrow, therefore facilitating two different particle count modes. The most common one is the single particle count mode, where each single light-scattering event of a particle in the optical sensor is counted individually. The single particle count mode breaks down at high concentration, where two or more particles may simultaneously be present in the sensor, resulting in a single combined light-scattering event. The two or more particles in the sensor would therefore be counted as a single particle, resulting in too low particle number concentrations reported by the CPC. This phenomenon is known as coincidence error. Depending on the CPC

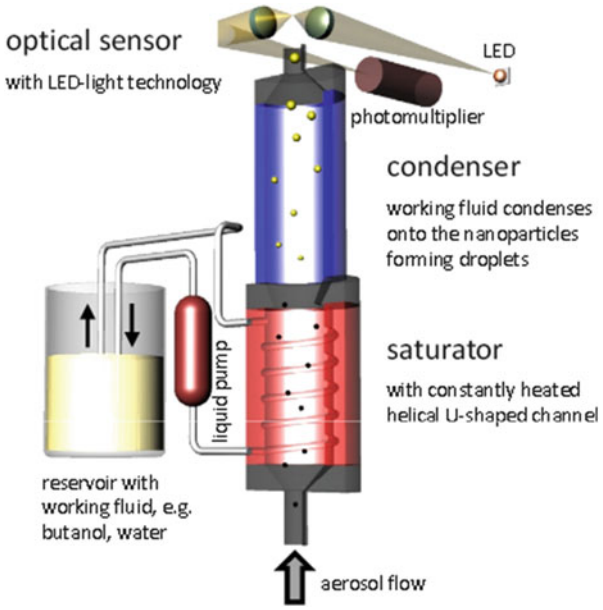

Fig. 2 Schematic of a condensation particle counter (CPC, image courtesy of Palas GmbH)

model, the upper concentration limit for the single particle count mode is typically between around 50,000 1/cm^3 and 300,000 1/cm^3, although some higher and lower exceptions apply. For higher concentrations, some instruments switch to a so-called photometric mode. In the photometric mode, the total light scattered by all particles in the optical sensor is quantified. If all droplets have the same size and refractive index, then each particle scatters the same amount of light and therefore the particle number concentration can be determined. The photometric mode extends the concentration range of a CPC up to between one and ten million particles per cubic centimeter. A prerequisite for the photometric particle count mode is that the droplet size is known and ideally material independent. The latter can only be assumed for alcoholic working fluids, whereas it was shown that the eventual droplet size in water-based CPCs can vary drastically in case of hydrophobic and hydrophilic particles [10]. If an average, material-independent droplet size is assumed for the calibration of water-based CPCs, the concentration measurements can be significantly biased.

The lowest particle sizes that can be detected with modern CPCs are between 2.5 and 10 nm (depending on model). For alcohol-based CPCs, the lower size limit only weakly depends on the particle material, whereas the activation of small particles with water vapor is different for hydrophilic and hydrophobic particles. The upper size limit of CPCs is usually not well specified. While in principle micron-sized particles would be more easily detectable in the sensor, they also get more easily lost in the instrument due to inertia or sedimentation. Most manufacturers therefore specify the upper limit as 1 μm, although there is no strict reason for a clear cutoff. It should, however, be noted that the number concentration of micron-sized

particles is typically very low (see Fig. 1). CPC instruments are available from several manufacturers including (in alphabetical order) Grimm Aerosol (Ainring, Germany), HCT (Korea), Palas (Karlsruhe, Germany), and TSI Inc. (Shoreview, MN, USA).

Measurement of Particle Lung-Deposited Surface Area Concentration

The lung-deposited surface area (LDSA) concentration is the only surface area-related metric that can currently be measured directly. The LDSA concentration is the fraction of the airborne particle surface area concentration that upon inhalation would deposit in the human lung. The LDSA concentration can be determined by measuring the number size distribution, weighting it with the particle surface area, i.e., πd_p^2 (see surface area size distribution in Fig. 1), and the lung deposition efficiency, before integrating it over the particle size range of interest. The lung deposition efficiency can be obtained for different compartments of the human lung from sampling conventions [11] or a model [12]. Since it is dependent on individual physiological and breathing parameters, a parameter set has been defined for a "reference worker" in order to make data comparable [13]. Available instruments determine the fraction that would deposit either in the alveolar or tracheobronchial region of the lung.

The first instrument to measure the LDSA concentration was the Nanoparticle Surface Area Monitor (NSAM, TSI model 3550) [13, 14]. The instrument is depicted in Fig. 3 and is to date the only stationary instrument that determines this metric. The aerosol is taken in at a flow rate of 2.5 L/min and passes a cyclone with 1 μm cutoff (not shown in the figure), before it is split into a 1 L/min ion jet flow and a 1.5 L/min aerosol flow. The ion jet flow passes a corona needle with an applied voltage of +2.5 kV. The high voltage at the corona tip establishes a corona discharge which generates ions. These ions are transported convectively with the ion jet flow into a mixing chamber, where it is recombined with the aerosol flow. Ions and particles collide due to Brownian motion, thereby charging the particles. Excess ions are removed in the downstream ion trap, before the particles are collected in a Faraday cup electrometer to measure the total particle-induced current. The number of elementary charges carried by the particles depends on the particle diameter d_p and scales with $d_p^{1.13}$ [15, 16]. It was assumed that at least for particles >20 nm, the LDSA follows the same particle size dependence [13, 14], so that a simple calibration factor is sufficient to obtain the LDSA concentration from the measured current. The LDSA of particles below 20 nm would be overestimated by the measurement of the current. The ion trap voltage can therefore be adjusted to not only remove ions but also certain amounts of highly mobile small particles in order to adjust the instrument's response to the required one for alveolar or tracheobronchial LDSA concentration for sub-20 nm particles. It was later shown that this measurement principle is only capable of measuring the LDSA concentration accurately up to 400 nm. The LDSA concentration of larger particles

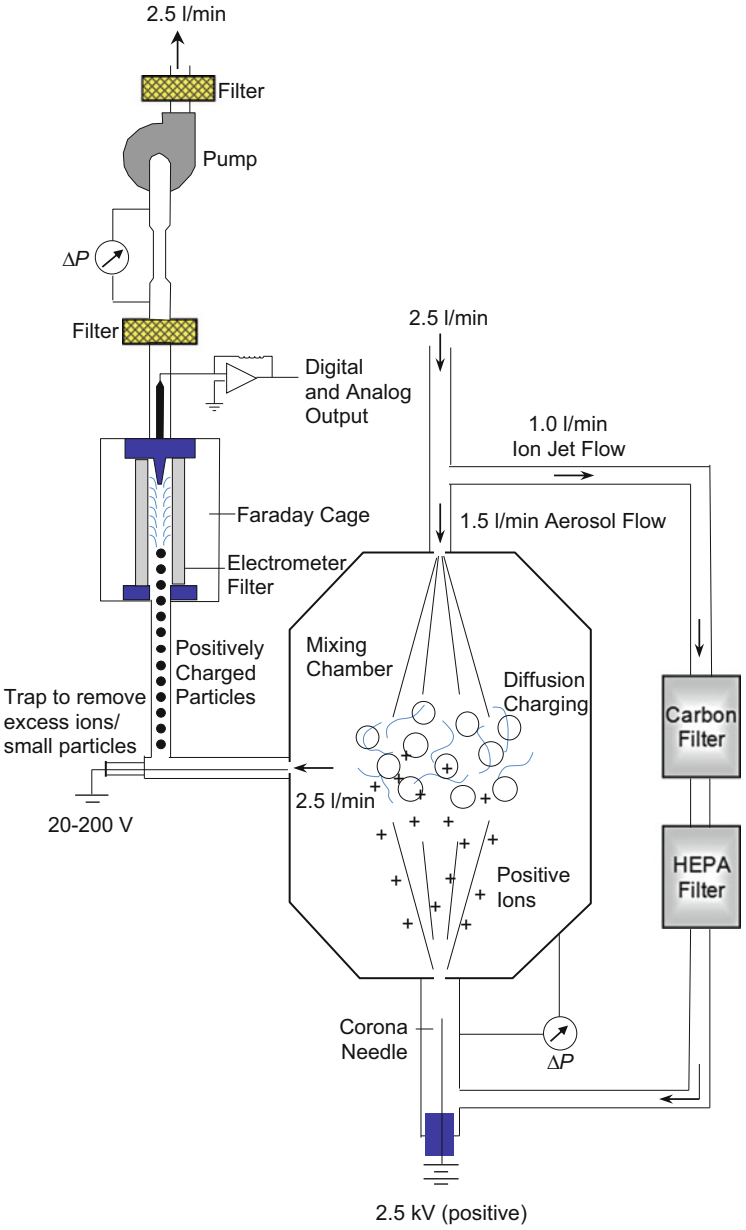

Fig. 3 Schematic of the Nanoparticle Surface Area Monitor (NSAM, TSI model 3550, image courtesy of TSI Inc.)

are drastically underestimated [17]. A corresponding new pre-separator with 450 nm cutoff and low pressure drop has been developed [18] but as of now has not yet been commercialized.

Measurement of Particle Mass Concentration

The tapered element oscillating microbalance (TEOM, Thermo Scientific) is an instrument that was designed to measure ambient particle mass concentrations. TEOM uses a filter, mounted on the tip of a hollow, tapered glass tube, which is clamped on the lower and free to vibrate on the upper end [19]. Two magnets are mounted on the sides of the glass tube near the upper end. An alternating magnetic field is applied, causing the upper end of the glass tube with the filter to vibrate at a frequency around 250 Hz. The excitation energy is constant, resulting in a constant vibration frequency as long as the mass of the system remains constant. The aerosol is drawn through the filter and the glass tube at an adjustable flow rate between 1 and 3 L/min. The particles deposit on the filter, thereby increasing its mass, causing the vibration frequency to decrease. The mass increase of the filter and hence the airborne particle mass concentration are determined from the frequency gradient. In principle, there is no upper or lower particle size limit for this method, but a minimum mass concentration needs to be available. As a rule of thumb, mass concentrations below approximately 5 $\mu g/m^3$ (equivalent to approximately 10,000 $1/cm^3$ of 100 nm particles with unit density) are no longer measurable. The particle size range can be limited at the upper end by the use of an impactor. Impactors with cutoff sizes of 10, 2.5, and 1 μm are available from the manufacturer, but none in the nano-range.

Measurement of Particle Size Distribution by Electrical Mobility Analysis

Electrical mobility analysis is the most common measurement method for the determination of number size distributions of submicron particles down to the nanometer range. The most accurate electrical mobility analyzer is the so-called scanning mobility particle sizer (SMPS) [20], which is an advancement of the earlier differential mobility particle sizer (DMPS) [21, 22]. SMPS and DMPS consist of four major components (see Fig. 4), i.e., an impactor to remove all particles that are too large, a neutralizer to charge the particles to a known bipolar charge distribution [23, 24], a differential mobility analyzer (DMA) [25] to classify the particles, and a condensation particle counter (CPC) to determine the concentration of the classified particles. The main advantage of SMPS over DMPS is its higher time resolution. While a DMPS takes about 15 min to complete the measurement of a size distribution, the SMPS only requires a few minutes. Since DMPS systems are no longer commercially available, only SMPS will be covered in the following. The SMPS is currently considered the state of the art and most accurate

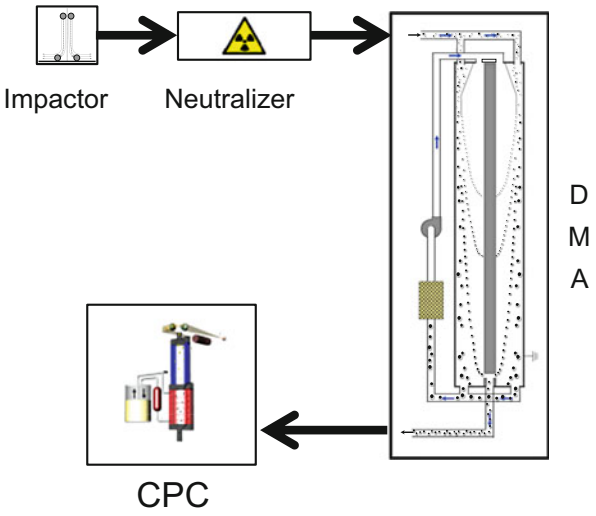

Fig. 4 Schematic of an SMPS and DMPS (CPC, image courtesy of Palas GmbH; DMA, image courtesy of TSI Inc.)

means for measuring number size distributions of airborne submicron particles [26, 27].

The DMA (see Fig. 5) is the key component of an SMPS. It classifies particles according to their electrical mobility Z_p:

$$Z_p = \frac{n \cdot e \cdot C_c(d_m)}{3\pi \cdot \eta \cdot d_m}. \tag{1}$$

In Eq. (1), d_m is the electrical mobility particle diameter, n is the number of particle-borne elementary charges e (1.602×10^{-19} As), C_c is the Cunningham slip correction factor [28, 29], and η is the gas viscosity. The electrical mobility diameter describes that the particle under consideration behaves in the electric field of the DMA like a spherical particle of this diameter. If the particle is spherical, the electrical mobility diameter equals the geometric sphere diameter, whereas in case of nonspherical particles, it is the diameter of an equivalent sphere.

The DMA is essentially a coaxial capacitor with an inner and an outer electrode. The charged test aerosol enters the DMA through an annular slit near the outer electrode and is separated from the inner electrode by a particle-free sheath flow. Typical aerosol flow rates are between 0.1 and 1.0 L/min with the sheath flow rate commonly by a factor of ten higher. At the bottom of the DMA, two flows are withdrawn, a monodisperse aerosol flow through a thin slit in the inner electrode and the remaining excess flow through the annular ring between inner and outer electrode. Usually the flow rate of the monodisperse aerosol flow equals the flow rate of the incoming polydisperse aerosol and the excess air flow is recycled as the sheath flow. If no voltage is applied between the inner and the outer electrode, the particles move along the outer electrode and no particles reach the monodisperse aerosol flow. If a voltage is applied, particles of one polarity (depending on

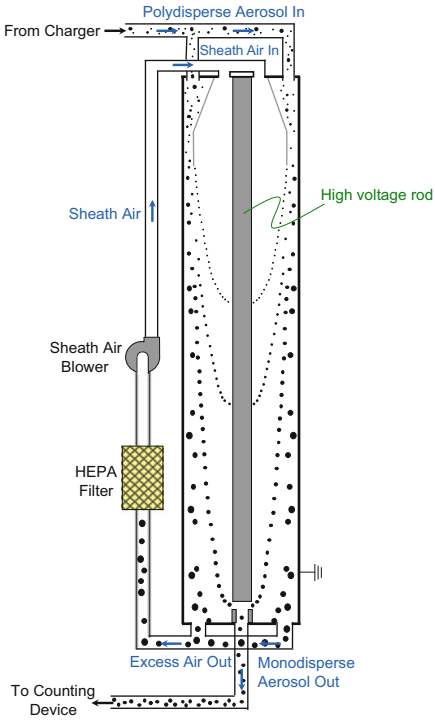

Fig. 5 Schematic of a differential mobility analyzer (DMA, image courtesy of TSI Inc.)

direction of the electric field) migrate toward the inner electrode at a velocity v_p, defined by the electrical mobility Z_p (see Eq. (1)) and the electric field strength E:

$$v_p = Z_p \cdot E. \tag{2}$$

For a given DMA voltage and thus electric field strength, only particles of a certain electrical mobility reach the slit for the monodisperse aerosol and are carried away with this flow. Particles with higher electrical mobility, i.e., smaller and/or higher charged particles, hit the inner electrode at a higher location, while particles with lower mobility are carried away with the excess flow. By changing the DMA voltage, the full range of electrical mobility can be scanned. In the SMPS, the voltage is continuously ramped, whereas in the DMPS it is increased in steps. All manufacturers offer DMAs with different column lengths to cover different particle size ranges, typically a long DMA [24, 30] to cover sizes between approximately 10 nm and 1,000 nm and a nano-DMA [31, 32] to extend the size range down to 2.5 nm or even below. The concentration of the mobility-classified particles is measured by a CPC downstream of the DMA. From Eq. (1), it is apparent that different combinations of particle size and number of elementary charges result in equal electrical mobility. Thus, the classified aerosol exhibits a multimodal size distribution with discrete peaks, each one representing a certain number of particle-borne elementary charges and the corresponding particle size. The primary output

of the SMPS is hence the number concentration of classified particles as a function of their electrical mobility. A complex data deconvolution routine [33] is used to obtain the number size distribution from the mobility distribution, taking into account the charge distribution the particles acquire in the neutralizer [23, 24], the diffusion losses of particles in the system and the DMA [34], the DMA transfer function [35], and the counting efficiency of the CPC [36, 37]. Due to its statistical data evaluation routine, the CPC needs to count a certain number of classified particles downstream of the DMA in each size channel. As a rule of thumb, size distributions with number concentrations below 1,000 1/cm^3 should be treated critically. The size distributions are delivered with resolutions up to 64 size channels per size decade. To make number size distributions measured with different size resolutions comparable, the concentration data usually gets normalized with respect to the size channel width, i.e., commonly as $dN/d\log(d_p)$. SMPS instruments are available from several manufacturers including (in alphabetical order) Grimm Aerosol (Ainring, Germany), HCT (Korea), Palas (Karlsruhe, Germany), and TSI Inc. (Shoreview, MN, USA). For a long time, the main downside of the SMPS was its need for a radioactive neutralizer (mainly ^{85}Kr or ^{241}Am). More recently, all SMPS manufacturers introduced soft X-ray neutralizers [38–40] as nonradioactive alternatives which require significantly lower bureaucratic efforts.

The fast mobility particle sizer (FMPS, TSI model 3091) is an alternative to the SMPS. It follows the same overall principle, i.e., electrical mobility analysis, but differs in numerous details. The main advantage of the FMPS over the SMPS is its high time resolution of 1 s. The high time resolution, however, comes at the price of reduced accuracy [26, 27] and size resolution. Figure 6 shows a schematic of the FMPS.

The aerosol is taken in at a flow rate of 10 L/min and first passes a (nonradioactive) unipolar corona charger to positively charge the particles, before it enters a coaxial classifier near the inner electrode. Inside the classifier, the aerosol flow is surrounded by a particle-free sheath flow at a flow rate of 40 L/min. A positive high voltage is applied to the inner electrode to repel the particles toward the outer electrode. The voltage is kept constant and therefore the location where the particles hit the outer electrode is a function of their electrical mobility. The outer electrode consists of an array of 22 electrode rings, electrically insulated from each other. Each electrode ring therefore represents a certain electrical mobility bandwidth and is connected to an electrometer which measures the current induced by the deposition of charged particles. A data deconvolution routine is used to determine the number size distribution from the current distribution, taking into account the charge distribution of the particles downstream of the corona charger. It is known that unipolar corona chargers have a charging efficiency which is proportional to approximately $d_p^{1.1}$ [15]. Taking into account that the Cunningham slip correction factor decreases very steeply with increasing particle size for particles smaller than around 100 nm, but gets a very weak function of the particle diameter for sizes >200 nm to eventually become constant, it is obvious from Eq. (1) that the dependence of the electrical mobility on particle size for particles larger than

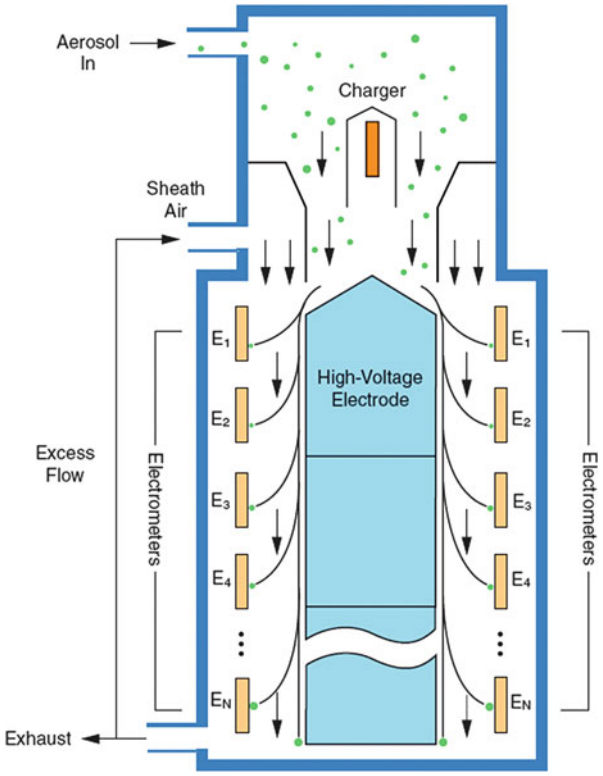

Fig. 6 Schematic of the fast mobility particle sizer (FMPS, TSI model 3091, image courtesy of TSI Inc.)

>200 nm gets increasingly weak and reaches a minimum around 400 nm [41]. Although the instrument is supposed to cover a size range from 5.6 to 560 nm, the sizing accuracy for particles larger than approximately 200 nm is rather poor [26, 27, 41], whereas the overall agreement for particle sizes below 100 nm is typically acceptable.

Measurement of Particle Size Distribution by Inertial Separation

Other instruments to obtain size-resolved information on airborne particles are cascade impactors. The process of inertial particle removal is known as impaction. In an impactor, the aerosol is first accelerated in a nozzle before it is diverted by 90° around an impaction plate. While small particles follow the streamlines, larger particles with high inertia divert from the streamlines and are deposited on the impaction plate (see Fig. 7).

Whether or not a particle is deposited by impaction can be determined by means of the dimensionless Stokes number *Stk*. The Stokes number is defined as the ratio of the stopping distance of a particle and the characteristic size of the flow obstacle.

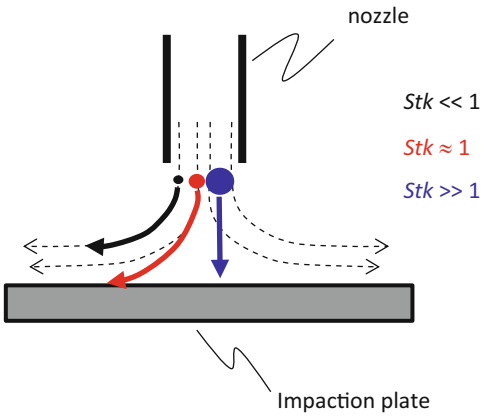

Fig. 7 Principle of an impactor

For $Stk << 1$, the particles follow the streamlines perfectly, whereas for $Stk >> 1$, the particles move straight, more or less independent of the flow direction. For an impactor with round nozzles, it is usually assumed that 50% of the particles get deposited in case of $Stk_{50} = 0.24$ [42]. The corresponding particle size d_{50}, at which 50% of the particles are deposited, is also referred to as the cutoff diameter. The cutoff diameter is a characteristic parameter of an impactor and can be determined by Eq. (3):

$$d_{50}\sqrt{C_c(d_{50})} = \left[\frac{9\pi \cdot \eta \cdot D_j^3 \cdot Stk_{50}}{4 \cdot \rho_p \cdot Q}\right]^{\frac{1}{2}}. \tag{3}$$

In Eq. (3), η is the gas viscosity, D_j is the nozzle diameter, ρ_p is the particle density, and Q is the flow rate. Since the collection efficiency depends not only on particle size but also on particle density (see Eq. (3)), the particle diameter is described as an aerodynamic equivalent diameter d_{ae}. The aerodynamic diameter describes that the (irregularly shaped) particle under consideration settles or impacts like a sphere with unit density ($\rho_0 = 1$ g/cm^3 = 1,000 kg/m^3) of this size. For a spherical water droplet, the aerodynamic diameter is the same as the droplet diameter. In case of two particles with identical sizes but with different densities, the particle with higher density has a larger aerodynamic diameter than the one with lower density:

$$d_{ae} = d_m \cdot \sqrt{\frac{\rho_p}{\rho_o}}. \tag{4}$$

As shown in Eq. (3), for a given flow rate, the cutoff size of an impactor can be varied by varying the nozzle diameter. A cascade impactor uses a multitude of sequential impaction stages with decreasing nozzle diameters, thus stage by stage decreasing the cutoff size. The particles collected on each impaction plate therefore

cover the size range defined by the cutoff size of the preceding and this stage. The impaction plates may be weighed before and after particle collection to determine the mass size distribution, or they can be analyzed chemically or by electron microscopy to obtain the size-resolved chemical composition or particle morphology, respectively. Most cascade impactors sample particles in the micron size range, although some exist that can collect particles down to a few nanometers (e.g., the multi-orifice uniform deposit impactor (MOUDI) from MSP, Shoreview, MN, USA). Since the inertia of particles scales with the particle mass, i.e., the particle size to the third power, nanoscale particles only have a very low inertia. In order to be able to capture them by impaction, the opposing drag force has to be lowered by reducing the pressure.

The electrical low-pressure impactor (ELPI or ELPI+, Dekati, Tampere, Finland [43]) uses a total of 13 impaction stages and an after-filter stage to collect particles with sizes between 6 nm and 10 µm. In order to collect such small particles, the last collection stage operates at a pressure of only 100 mbar. In contrast to conventional cascade impactors, ELPI first charges the particles in a unipolar charger, and each impaction stage is connected to a sensitive electrometer to measure the current induced by the collected particles as shown in Fig. 8. With the known charge distribution downstream of the unipolar charger, the number size distribution is determined from the measured current distribution. The time resolution of ELPI is variable and can be up to 0.1 s if the particle concentration is sufficiently high for the measured currents to be well above the electrometer noise level. ELPI is

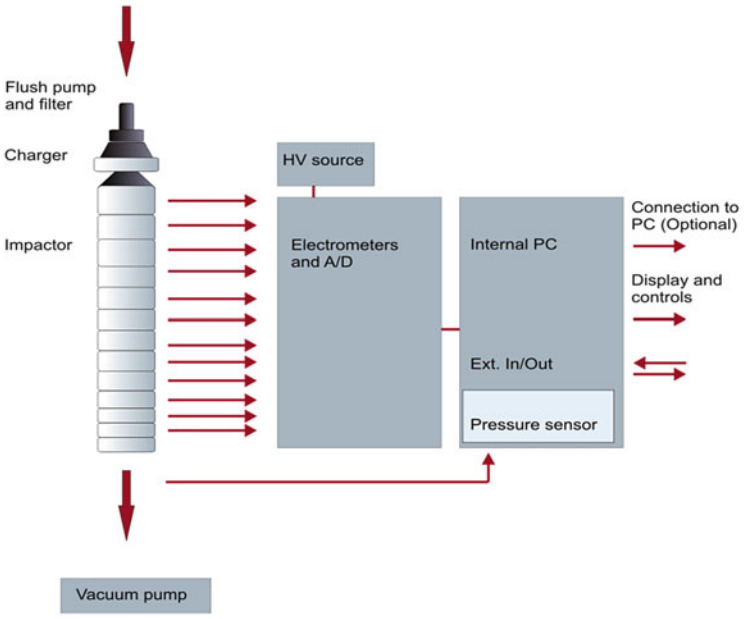

Fig. 8 Schematic of the electrical low-pressure impactor (ELPI or ELPI+, Dekati, Finland, image courtesy of Dekati)

currently the only instrument available that measures particle size distributions from a few nanometers up to 10 µm based on the same measurement principle, thus bypassing the challenge of converting size distributions based on different equivalent diameters. After sampling, the impaction plates are available for further analyses, for example, concerning the particle morphology or chemical composition.

2.1.2 Time-Integrating Instruments

Time-integrating instruments are used to collect particles over a certain time for subsequent analyses. Different collection mechanisms and substrates are used. The main collection mechanisms are filtration as well as electrostatic and thermal collection. Substrates need to be chosen to be suitable for the subsequent analysis. The only main size-resolving sampling technique is the cascade impactor, which is described in the section on the electrical low-pressure impactor above. All other time-integrating samplers do not deliver particle size-resolved samples; however, depending on the substrate and analysis, size-resolved information may be obtained, for example, through electron microcopy. In most cases, the size range of the collected particles may be limited at the upper end by the use of an appropriate upstream impactor.

Filter Sampling

Filter samplers are rather simple devices, in which the aerosol is drawn through a filter at a known flow rate to collect the particles. Depending on the planned analysis, fiber or membrane filters are used. Fiber filters are typically used to determine the average particle mass concentration by weighing the filter prior to and after sampling. The filters can subsequently also be used for chemical analyses of the collected particles, for example, by inductively coupled plasma mass spectrometry (ICP-MS) or by thermal analysis for elemental and organic carbon (EC-OC analysis) [44]. Alternatively, membrane (e.g., Nuclepore) filters can be used if the particles are to be collected on the filter surface. In this case, they can, for example, be washed off more easily. The resulting suspension can then be analyzed, for example, by electron spin resonance spectroscopy for the potency of the particles to generate reactive oxygen species (ROS) [45]. The potency of particles to generate ROS is an indicator that the particles may cause lung inflammation upon inhalation. Chen et al. [46] used membrane filters to eventually evaluate the particle size distribution of the collected agglomerates and aggregates by electron microscopy. With the help of a particle deposition model for the membrane filter, the size distribution of the particles in the airborne state is reconstructed.

Filter samplers are typically used in combination with an impactor upstream to limit the particle sizes to a maximum of 10 µm (PM_{10}), 4 µm (respirable fraction), 2.5 µm ($PM_{2.5}$), or 1 µm (PM_1).

Electrostatic Sampling

If a charged particle is exposed to an electric field, a Coulomb force makes the particle move in direction or counter direction (depending on polarity of the net particle charge) of the electric field (see Eq. (2)). In a DMA (see Fig. 5), this phenomenon is used to classify particles, but it can also be utilized to collect charged particles on a substrate in an electrostatic precipitator. The commercially available stationary ESPs collect incoming particles on a flat substrate inside a metallic cup. A schematic of an electrostatic precipitator for particle sampling is shown in Fig. 9. This concept is realized in the Grimm electrostatic precipitator (Grimm Aerosol model 5.561) and the TSI nanometer aerosol sampler (NAS, TSI model 3089). The aerosol enters the ESP through a circular inlet in the top of the housing at a flow rate between 1 and 5 L/min, flows around the inner electrode with the substrate, and is discharged through the outlet in the bottom. The outer housing of the ESP is grounded and a high positive or negative potential is applied to the inner electrode, thereby establishing an electric field between the inner and outer electrode, which drives the particles onto the surface of the substrate, where they are collected [47]. Typical substrates include semiconductor (silicon or gallium arsenide) wafers or wafer chunks, TEM grids, or glassy carbon. The spot size of the collected particles can be adjusted by adjusting the collection voltage. Semiconductor wafers have perfectly flat surfaces and are therefore well suited for scanning electron microscope (SEM) analyses. TEM grids are used for transmission electron

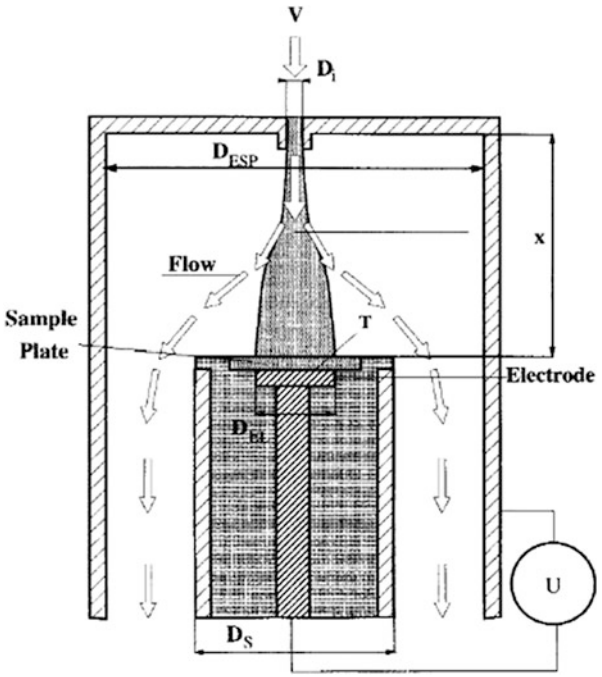

Fig. 9 Schematic of an electrostatic precipitator (from [48])

microscope (TEM) analyses. In both cases, the particles can be analyzed for their sizes and morphologies or in combination with electron dispersive X-ray (EDX) spectroscopy for their chemical composition. While TEM is able to analyze the substrates with higher resolution than SEM, the use of an SEM is easier and less cost intensive. For electron microscopic analyses, it is necessary not to overload the substrates to avoid that particles deposit on top of each other, thereby becoming indistinguishable. A wider deposition spot size is therefore preferred, which can be achieved by choosing a relatively low collection voltage. Glassy carbon substrates are used to collect particles for subsequent total X-ray fluorescence (TXRF) spectroscopy [48]. TXRF requires the particles to be collected in a small spot, which is achieved by a high collection voltage.

The commercially available stationary ESPs are designed to collect monodisperse particles downstream of a DMA (see Fig. 5). Since particles leaving a DMA are always charged, the ESPs do not contain means for particle charging. If these ESPs are used for sampling unclassified polydisperse particles, one may rely on the natural charge of airborne particles. Once airborne, particles interact with the ubiqituous air ions. Aged airborne particles are therefore usually charged according to a Boltzmann distribution, i.e., with more or less equal amounts of positive and negative charges. Only particles of one polarity would then be collected in the ESP. Alternatively, a unipolar charger can be used upstream; however, as of now, no commercial solution is available.

2.2 Portable Equipment

Portable measurement equipment is characterized by its ability to measure independent of mains power and by its smaller size compared with stationary equipment. Portable instruments are sufficiently mobile to be easily moved between different measurement locations and are therefore suitable for measurements according to tier 2 in tiered workplace exposure assessment. Portable equipment typically has a lower accuracy and lower sizing resolution than stationary equipment. The measurement methods of portable instruments are all the same or very similar to the ones described above for the stationary equipment and are therefore not repeated here. Instead, the instruments are only briefly introduced.

2.2.1 Time-Resolving Instruments

Measurement of Particle Number Concentration

Handheld condensation particle counters (handheld CPCs) are available to measure the particle number concentration of airborne particles. These handheld CPCs use isopropyl alcohol (IPA) as working fluid and are battery operable. During operation, the handheld CPCs have to be maintained in a horizontal orientation to avoid

flooding of the optics with IPA. Depending on model, their lower size limit is 10 nm (TSI CPC model 3077, Kanomax model 3800) or 20 nm (TSI P-Trak), respectively. Their concentration range is nominally limited to 100,000 1/cm^3 in case of TSI model 3077 and Kanomax model 3800 and 500,000 1/cm^3 in case of TSI P-Trak. Above this limit, coincidence errors may occur, resulting in too low concentrations being reported by the CPCs. However, no alarm is given in this case. The TSI model 3077 was shown to be accurate to within ±5% [49] as long as the instrument is well calibrated and the concentrations are within the instrument's specified concentration range. More recently, it was found that the TSI P-Trak seems to show coincidence errors already for concentration higher than 100,000 1/cm^3 [50], despite the much higher specified concentration limit.

Other instruments that may be considered portable number concentration measuring instruments are based on diffusion charging, such as the DiSCmini (Testo GmbH, Titisee-Neustadt, Germany [51]) or NanoTracer (Oxility, Eindhoven, the Netherlands [52, 53]). These instruments are, however, small enough that they can also be used as personal measuring instruments and are therefore described below in the section on personal measurement equipment.

Measurement of Lung-Deposited Surface Area Concentration

The Nanoparticle Surface Area Monitor (NSAM, TSI model 3550; see above) has been downsized and differently packaged to make the instrument smaller, portable, and battery operable. This instrument has been commercialized by TSI as Aerotrak 9000. It is essentially the same instrument as NSAM and shows a similar accuracy [17] and comparability.

Other instruments that can be considered as portable devices for the measurement of LDSA concentrations are DiSCmini and NanoTracer and are described below under personal measurement equipment.

Measurement of Particle Size Distribution

Portable instruments for the measurement of submicron particle number size distributions have rather recently entered the market. They are all based on electrical mobility analysis and are in principle very similar to the SMPS described above. All these instruments are able to operate on battery power for several hours and independent of an external computer.

The portable aerosol mobility spectrometer (PAMS, Kanomax) follows the same but miniaturized setup as the SMPS (see Fig. 4) with the main exception that the neutralizer is a bipolar corona charger which provides a similar charge distribution like a radioactive or soft X-ray charger. The following DMA is of the radial type [54], i.e., it consists of two parallel circular electrodes. The aerosol and the sheath flow enter the space between the electrodes from outside and are discharged through central holes in the top and bottom electrode, respectively. The

monodisperse aerosol is guided to a CPC, which is basically the Kanomax handheld CPC, incorporated into the system. PAMS can be operated in two flow rate modes. With an aerosol flow rate of 0.2 L/min, it measures the size distribution in a size range from 14.5 to 863 nm in ≥42 s and with 0.4 L/min in a range from 10 to 433 nm in ≥81 s.

The TSI NanoScan (model 3910) [55] follows essentially the same setup as PAMS but uses a unipolar corona charger to replace the radioactive neutralizer. NanoScan determines the number size distribution of airborne particles, nominally in a size range from 10 to 420 nm with a time resolution of 60 s. The unipolar charger has a similar particle charging characteristic like the unipolar charger used in the FMPS (see above) and therefore gives rise to the same challenges in the electrical mobility analysis of particles larger than approximately 200 nm, due to the increasingly weak dependence of the electrical mobility on particle size. This phenomenon has been shown experimentally [56]. It was found that the sizes of a polydisperse DEHS aerosol with a 200 nm modal diameter were significantly underestimated by NanoScan. The number concentration of a NaCl aerosol with 10 nm modal diameter was drastically underestimated by NanoScan in the same study. Measurements with other aerosols with modal diameters between 10 and 200 nm delivered satisfying results. Stabile et al. [57] found acceptable agreement of NanoScan size distributions with those measured by SMPS, but they reported significant deviations for agglomerated particles.

The nano-ID NPS500 (Naneum, Canterbury, UK) determines size distributions in a size range from 5 to 500 nm with a time resolution of ≥30 s. It uses a patented unipolar corona charger and a planar DMA [58]. The charger limits the number of multiple charges on the particles which simplifies the data deconvolution. The design of the electrical mobility classifier is not disclosed. The CPC operates on a patented organic working fluid, which allows for a very long operation of up to months without the need for a refill.

Grimm Aerosol (Ainring, Germany) follows a different concept for their portable particle sizer. In the mini-wide range aerosol spectrometer (mini-WRAS, model 1.371), they combine an optical spectrometer to optically measure the number size distribution in a particle size range from 200 nm to 35 μm with a simplified electrical mobility analyzer to extend the measurement range down to 10 nm. Inside the electrical mobility classification part, the incoming aerosol is charged in a unipolar corona charger, followed by a concentric electrical mobility classifier. Unlike in a DMA, the classifier operates without sheath flow. Instead, the current from all charged particles leaving the classifier is measured with a downstream electrometer. By increasing the voltage in the classifier, an increasing amount of particles is removed from the aerosol and deposited inside the classifier. Due to the size dependence of the electrical mobility, the current gradient as function of classifier voltage can be tracked back to the particle number size distribution.

The eventual size distribution is delivered with a total size resolution of 40 size channels, ten from the electrical and 30 from the optical measurement.

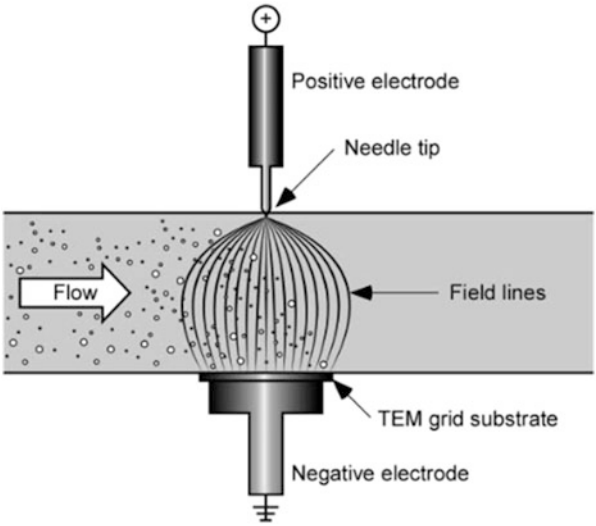

Fig. 10 Schematic of ESPnano model 100; image from [59]

2.2.2 Time-Integrating Instruments

A novel, commercial handheld ESP is available from ESPnano (model 100, ESPnano, Spokane, WA, USA [59]). The sampler is small and battery operated and collects airborne particles onto TEM grids. A schematic of the ESP is shown in Fig. 10. The sampler is intended to be used mainly in workplace exposure assessment to take samples in locations, where a release of particles is suspected. The TEM analysis can then provide proof for the presence or absence of a certain, for example, critical substance.

The ESPnano model 100 uses a unipolar corona charger to generate ions near a tip electrode. When a positive high voltage is applied to the tip, a corona is formed that ionizes the air. The tip electrode faces the sampling electrode with the TEM grid. Consequently, the generated ions follow the electric field lines into the perpendicular aerosol flow, where they collide with the particles to charge them. The charged particles are deposited onto the TEM grid within the same electric field that is used to generate the ions and charge the particles. As the device is intended to be used under field conditions, a removable "key" system was designed that would insure a fast and easy replacement of the sample media between different samplings. The sample media can be pre-loaded in the lab onto the key, and after sample collection, the key can be kept in airtight holders until the sample analysis is performed.

2.3 Personal Equipment

Personal measurement equipment is characterized, similar to portable measurement equipment, by its ability to measure independent of mains power. Additionally, the devices should be sufficiently small, lightweight, and robust so that they could be worn by a worker over an 8-h shift and would not interfere or affect with any of the activities carried out by the worker. They should also be easy to use for nonspecialist personnel. Only very recently, nanospecific personal samplers and monitors have become available that are capable of measuring different metrics, i.e., number concentration and mean particle size, LDSA concentration, mass concentration, etc., in the breathing zone of a human. As most of them are available only as prototypes, only the commercially available ones will be described and some additional examples of prototypes will be mentioned. An overview of the working principles of the personal monitors is given in Fig. 11.

2.3.1 Time-Resolving Instruments

Measurement of Number Concentration, Lung-Deposited Surface Area Concentration, and Mean Particle Size

The DiSCmini (Testo GmbH, Titisee-Neustadt, Germany), as well as its original prototype, the miniDiSC (University of Applied Sciences and Arts Northwestern Switzerland, Windisch, Switzerland), is a portable, battery-operated instrument that determines the alveolar LDSA concentration, number concentration, and mean particle size with a time resolution of 1 s [51]. The instrument draws the test aerosol at a flow rate of 1 L/min through an optional impactor, where particles larger than 700 nm are removed. The remaining particles pass through a positive unipolar diffusion charger, acquiring an average charge that is approximately proportional to the particle diameter. Then the charged particles pass through an ion trap where the excess ions are removed and finally a dual-stage particle deposition system. The first stage consists of a stack of stainless steel grids where preferentially small particles are deposited due to Brownian diffusion. The second stage consists of a high efficiency filter, where the remaining particles are collected. Both stages are connected to Faraday cup electrometers that continuously measure the current induced by the deposited particles (see Fig. 11 for the schematic of the working principle). With these two independent measurements, the mean particle size and the total particle number concentration can be determined from the ratio and the sum of the currents by assuming a lognormal particle size distribution with a geometric standard deviation of $\sigma_g = 1.9$. In addition, the total current, i.e., the sum of the currents from both stages, is proportional to the lung-deposited surface area concentration, as from approximately 20–400 nm the LDSA and the charging efficiency of the DiSCmini charger follow nearly the same size dependence and can therefore be determined by applying a simple calibration factor.

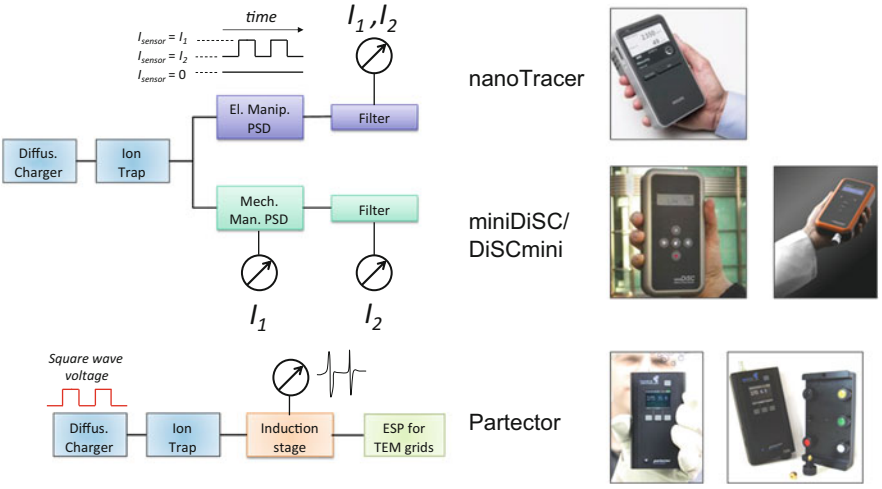

Fig. 11 Schematic of the working principle of the diffusion charger-based monitors: NanoTracer (*top*), DiSCmini/miniDiSC (*middle*), and Partector (*bottom*)

Another portable instrument based on the unipolar diffusion charging of particles is the NanoTracer (discontinued by Philips Aerasense, Eindhoven, the Netherlands, recently licensed by Oxility, Eindhoven, the Netherlands). The instrument draws the aerosol at a flow rate between 0.3 and 0.4 L/min, and after charging the particles in a unipolar corona charger, these pass in between two parallel electrodes, to which a square wave voltage is applied [52]. As long as the voltage is zero, no particles are removed and a very sensitive electrometer downstream of the electrode system measures the charge of all particles. When a certain voltage is applied to the electrodes, a fraction of small particles with high electrical mobility deposits on the electrodes and subsequently a lower current is measured by the electrometer. The alveolar LDSA concentration is determined from the current measured during zero-voltage phases. The number concentration and mean particle size are derived from the two different currents measured during high and zero voltage applied to the precipitator, respectively. The NanoTracer can operate in two different modes: fast mode, when, by assuming a mean particle size equal to 50 nm, the particle number concentration is being measured in real time (3 s), and advance mode (minimum time resolution 16 s), when both particle number concentration and averaged particle size are being determined. Only newer versions of the NanoReporter software (e.g., 1.1.0.96) permit the evaluation of NanoTracer data for LDSA concentration [53].

The DiSCmini and the NanoTracer are not small enough to directly sample in the breathing zone of an individual, but they can be worn on a belt and take aerosol samples from the breathing zone through a flexible tube.

Measurement of Lung-Deposited Surface Area Concentration

Partector is a small battery-operated personal monitor that determines the LDSA concentration with a time resolution of 1 s and is small enough to directly sample in the breathing zone of a worker. The aerosol is drawn in at 0.5 L/min, then passes a unipolar diffusion charger, followed by an ion trap and an induction stage, where the particle charge is detected with a Faraday cup electrometer [60]. When there is a temporal charge gradient in the induction stage, a current spike is induced with a magnitude proportional to the charge gradient. In order to trigger these charge gradients, the unipolar charger is operated with a square wave voltage, i.e., it gets intermittedly switched on and off with a frequency of 10 Hz. In consequence, a periodic signal is measured at the electrometer, the amplitude of which is determined in the instrument. The amplitude of this signal is proportional to the charge carried by the aerosol pulses and can therefore be calibrated to correspond to the LDSA concentration in the alveolar region of the lung of a reference worker, which is what the instrument reports.

The recent enhancement of the personal monitor, the Partector TEM sampler, combines the Partector with an electrostatic precipitator that deposits particles on standard TEM grids. Because the particle concentration is measured online, the sampler automatically determines the optimal probe sampling time and stops sampling when a sensible coverage of the grid is reached (~1% of the area covered with particles).

A study conducted on the accuracy and comparability of these diffusion-charging electrical aerosol monitors showed that as long as the measured particle sizes are between 20 and 400 nm, the LDSA concentrations reported by the instruments can be measured with an accuracy of ±30%. The LDSA concentrations of particles smaller than 20 nm are overestimated, whereas the LDSA concentrations of particle >400 nm are underestimated [17].

2.3.2 Time-Integrating Instruments

Thermophoretic Sampling

The thermal precipitator sampler (TPS, RJ Lee Group, Monroeville, PA, USA) uses the thermophoretic force to collect nanoparticles onto standard TEM grids, for subsequent analysis of particle size, concentration, and chemical composition [61]. The sampler collects airborne particles by applying a relatively large temperature gradient to a narrow flow channel. Because of the temperature gradient, gas molecules on the hotter side of the particle have greater kinetic energy than those on the colder side, transfering more net momentum per collision to the particle than do molecules on the colder side, causing a thermophoretic force. The particles will move in the direction of decreasing temperature and will eventually deposit onto the colder side of the flow channel which includes the TEM grid.

Fig. 12 The thermal precipitation sampler (TPS): the overall device including the removable sample cartridge (*left*). *Right*: view of the TPS region containing the hot plate (**a**), TEM grid holder (**b**), and cold plate (**c**) [61]

The TPS samples aerosol at a flow rate between 1 and 10 mL/min and utilizes a removable sample cartridge that holds a hole-free carbon film supported by a 200-mesh nickel TEM grid onto which particles are deposited. The cartridge can be slid into the TPS body for sampling immediately below the hot plate while maintaining thermal contact with the cold plate to establish the thermophoresis zone (see Fig. 12). Because nickel is ferromagnetic, the grid is held in place by a small magnet located between the cold plate and the grid itself.

A transfer function was developed that relates the number, size, and composition of the collected particles to the ones of the test aerosol [62]:

$$N(d) = \left[\frac{x(d)A}{QtS}\right]\left[\frac{F(d)}{Pt(d)\eta(d)}\right]. \tag{5}$$

In Eq. (5), $x(d)$ is the number of particles with size d counted in a microscope field with area S and the total area of the substrate is A; $F(d)$ is a normalization factor that adjusts for known and unknown factors, e.g., any differences in the particle deposit between the field examined and the entire collection substrate; $Pt(d)$ is the fractional penetration of the particles through the sampler inlet; $\eta(d)$ is the fractional collection efficiency for these particles onto the sampler substrate; Q is the flow through the sampler; and t is the sampling time.

Also the first prototypes of another thermal precipitator, designed as a personal sampler for nanomaterials, have been built [63, 64].The TP samples thermophoretically particles onto silicon substrates that can be used for consecutive SEM/EDX analysis. The sampler has been evaluated and validated up to a size of 300 nm using monodisperse polystyrene latex (PSL) particles as well as soot particles.

Sampling on Different Filtration Media

The NanoBadge (NanoInspect, Alcen Group, France, and French Alternative Energies and Atomic Energy Commission) is a lightweight battery-operated portable device which collects airborne particles in the breathing zone of the worker (Fig. 13).

Fig. 13 The NanoBadge; the white cassette on the top of the device is equipped with a sealed track-etched membrane to collect airborne particles; a single on-off switch makes the device robust and very simple to use

The sampler is connected to a cassette, whose filter is analyzed offline by X-ray fluorescence spectroscopy (XRF), providing a cumulative mass-based quantification of the chemical elements present on the filters. Track-etched membranes are used to collect particles for subsequent analysis of particle size (SEM), elemental composition, and concentration (XRF). The sampler can be equipped with a pre-separator with a cutoff diameter of 4 μm (respirable fraction) to remove coarse particles. The NanoBadge 2013 version is operated with a flowrate of 0.6 L/min while the 2015 version is operated at 1 L/min. For both versions, the flow rate is kept in the range of ±5% over more than 10 h.

The measurement of the engineered nanoparticles' concentration by their constitutive element using XRF represents a very powerful strategy, because it is a way to get rid of the existing high and fluctuating background level of natural and anthropogenic nanoparticles. Moreover, it is a nondestructive analytical technique, meaning that the same sample can be characterized further with other techniques such as scanning electron microscopy (SEM). After sampling, the cassettes are extracted from the NanoBadge and sent directly to the service provider (NanoInspect) for analysis and subsequent data restitution (i.e., elemental mass concentration in the breathing zone averaged over the total sampling time).

The sampler has been evaluated and validated up to a size of 200 nm using ZnO and TiO_2 particles. The highly sensitive XRF technique yields the elemental composition of the collected particles with sensitivity in the order of a few tens of nanograms per filter and consequently could be used either over a full shift (e.g., 8 h) or during short operations (e.g., 15 min) to detect acute exposure events [65].

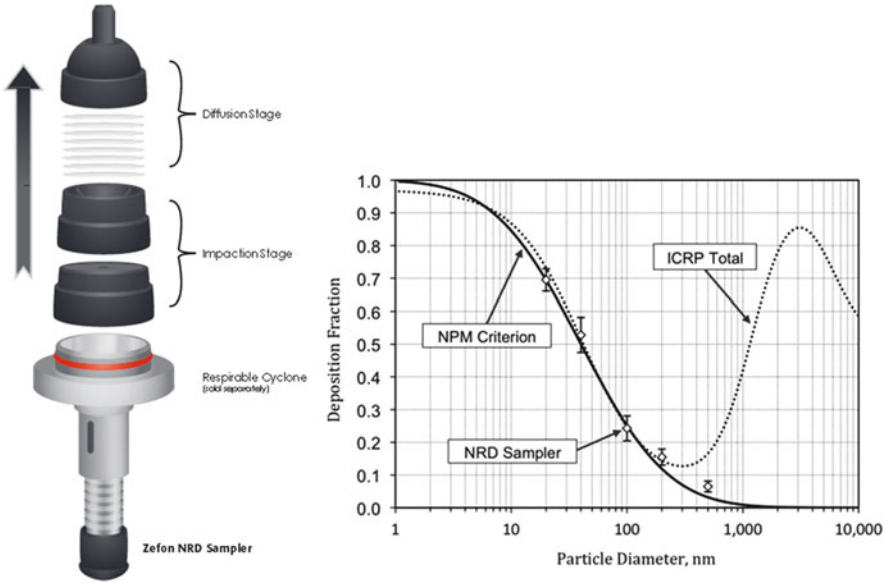

Fig. 14 Schematic of the NRD (*left*); NPM sampling criterion, ICRP total respiratory deposition, and effective deposition on the diffusion stage of the NRD sampler (*right*) [66]

The personal nanoparticle respiratory deposition (NRD, Zefon International, Ocala, FL, USA) [66] sampler was developed to be used as a full-shift personal sampler that selectively collects nanoparticles in a workplace atmosphere. To do this, firstly a new collection criterion, namely, the nanoparticulate matter (NPM), was devised in order to get the target collection efficiency of the sampler. The NPM is the fraction of airborne particles that would deposit in the human respiratory tract by Brownian diffusion. Based on this criterion, the NRD sampler would collect all particles smaller than 300 nm, the minimum deposition for submicrometer particles, that when inhaled can deposit anywhere in the respiratory tract (see Fig. 14).

The sampler operates at 2.5 L/min and consists of a respirable aluminum cyclone used to eliminate particles larger than 10 μm, followed by an impaction plate where particles larger than 300 nm are collected and a diffusion stage containing eight hydrophilic nylon mesh screens with 11 μm pore size and 6% porosity that collect particles with an efficiency that matches the NPM criterion.

The particles collected on the nylon fibers of the mesh screens can be characterized either by chemical analysis or by scanning electron microscopy to determine the size, number, and chemical composition of the collected particles.

Other examples of samplers designed for the evaluation of the personal exposure to nanoparticles, available only in the form of prototypes, are the $PM_{0.1}$ personal sampler [67] and the personal nanoparticle sampler (PENS) [68].

The $PM_{0.1}$ personal sampler consists of a commercially available two-stage precut impactor used to remove particles in the micron size range ($PM_{1.4}$-TSP), followed by a precut inertial filter that uses webbed stainless steel (SUS-316L)

fibers to remove fine particles ($PM_{0.5}$–$PM_{1.4}$) and a layered mesh inertial filter used for the $PM_{0.1}$ separation. The layered mesh inertial filter consists of commercially available mesh copper TEM grids sandwiched between copper spacers and has the advantage that these provide a uniform structure of fibers aligned perpendicular to the flow direction, maximizing the inertial effect on particles with less pressure drop and no loss in separation performance. By immersing the TEM grids in an appropriate solution, the collected particles can be extracted for chemical analysis.

The personal nanoparticle sampler (PENS) enables the collection of both respirable particulate mass (RPM) and nanpoarticles simultaneously at a flow rate of 2 L/min. It consists of a respirable cyclone, used to remove particles larger than 4 μm in aerodynamic diameter; a micro-orifice impactor, with a d_{pa50} of 100 nm; and a filter cassette containing a 37 mm Teflon filter. The micro-orifice impactor consists of a fixed micro-orifice plate with 137 nozzles of 55 μm inner diameter and a silicone oil-coated Teflon filter substrate rotating at 1 rpm to achieve a uniform particle deposition and avoid solid particle bouncing. Particles ranging from 4 μm down to 100 nm are collected on the impaction plate of the micro-orifice impactor, while nanoparticles are collected on the filter of the final stage. The performance of the sampler was evaluated in three metalworking plants during a day shift of 6–8 h and showed good accuracy with respect to the reference SKC respirable dust aluminum cyclone, regardless of the particle type [69].

References

1. European Commission (2015) Definition of a nanomaterial. http://ec.europa.eu/environment/chemicals/nanotech/faq/definition_en.htm. Accessed 20 Apr 2015
2. Johnston HJ, Hutchinson G, Christensen FM, Peters S, Hankin S, Stone V (2010) A review of the in vivo and in vitro toxicity of silver and gold particulates: Particle attributes and biological mechanisms responsible for the observed toxicity. Crit Rev Toxicol 40:328–346
3. Oberdörster G (2000) Toxicology of ultrafine particles: in vivo studies. Phil Trans R Soc A 358:2719–2740
4. Xia T, Kovochich M, Brant J, Hotze M, Sempf J, Oberley T, Sioutas C, Yeh JI, Wiesner MR, Nel AE (2006) Comparison of the abilities of ambient and manufactured nanoparticles to induce cellular toxicity according to the oxidative stress paradigm. Nano Lett 6:1794–1807
5. Driscoll KE (1996) Role of inflammation in the development of rat lung tumors in response to chronic particle exposure. Inhal Toxicol 8(Suppl.):139–153
6. Bruch J, Landsiedel R, Ma-Hock L, Pauluhn J, Ragot J, Wiemann M (2009) In vivo test systems, NanoCare – Health related aspects of nanomaterials, final scientific report; Chap 4.4, pp 48–67. http://nanopartikel.info/files/projekte/NanoCare/NanoCare_Final_Report.pdf. Accessed 30 Apr 2015
7. Poland CA, Duffin R, Kinloch I, Maynard A, Wallace WAH, Seaton A, Stone V, Brown S, MacNee W, Donaldson K (2008) Carbon nanotubes introduced into the abdominal cavity of mice show asbestos-like pathogenicity in a pilot study. Nat Nanotechnol 3:423–428
8. Standard EN1540:2011 (2012) Workplace exposure. Terminology. ISBN 978-0-580-70841-1
9. McMurry P (2000) The history of condensation nucleus counters. Aerosol Sci Technol 33:297–322

10. Keller A, Tritscher T, Burtscher H (2013) Performance of water-based CPC 3788 for particles from a propane-flame soot-generator operated with rich fuel/air mixtures. J Aerosol Sci 60:67–72
11. Vincent J (2005) Health-related aerosol measurement: a review of existing sampling criteria and proposals for new ones. J Environ Monit 7:1037–1053
12. International Commission for Radiological Protection (ICRP) (1994): Publication 66: Human respiratory tract model for radiological protection. Ann ICRP 24:1–3
13. Fissan H, Neumann S, Trampe A, Pui DYH, Shin WG (2007) Rationale and principle of an instrument measuring lung deposited nanoparticle surface area. J Nanopart Res 9:53–59
14. Shin W, Pui DYH, Fissan H, Neumann S, Trampe A (2007) Calibration and numerical simulation of nanoparticle surface area monitor (TSI model 3550 NSAM). J Nanopart Res 9:61–69
15. Jung H, Kittelson DB (2005) Characterization of aerosol surface instruments in transition regime. Aerosol Sci Technol 39:902–911
16. Kaminski H, Kuhlbusch TAJ, Fissan H, Ravi L, Horn HG, Han HS, Caldow R, Asbach C (2012) Mathematical description of experimentally determined charge distributions of a unipolar diffusion charger. Aerosol Sci Technol 46:708–716
17. Todea AM, Beckmann S, Kaminski H, Asbach C (2015) Accuracy of eletrical aerosol sensors measuring lung deposited surface area concentrations. J Aerosol Sci. in press, http://dx.doi.org/10.1016/j.jaerosci.2015.07.003
18. Asbach C, Fissan H, Kaminski H, Kuhlbusch TAJ, Pui DYH, Horn HG, Hase T (2011) A low pressure drop preseparator for eliminiation of particles larger than 450 nm. Aerosol Air Qual Res 11:487–496
19. Patashnick H, Rupprecht EG (1991) Continuous PM-10 measurements using the tapered element oscillating microbalance. J Air Waste Manag Assoc 41:1079–1083
20. Wang SC, Flagan RC (1990) Scanning electrical mobility spectrometer. Aerosol Sci Technol 13:230–240
21. Fissan HJ, Helsper C, Thielen HJ (1983) Determination of particle size distributions by means of an electrostatic classifier. J Aerosol Sci 14:354–357
22. Kousaka Y, Okuyama K, Adachi M (1985) Determination of particle size distribution of ultrafine aerosols using a differential mobility analyzer. Aerosol Sci Technol 4:209–235
23. Fuchs NA (1963) On the stationary charge distribution on aerosol particles in bipolar ionic atmosphere. Geofisica pura e applicata 56:185–193
24. Wiedensohler A (1988) An approximation of the bipolar charge distribution for particles in the submicron size range. J Aerosol Sci 19:387–389
25. Liu BYH, Pui DYH (1974) A submicron aerosol standard and the primary absolute calibration of the condensation nuclei counter. J Colloid Interface Sci 47:155–171
26. Asbach C, Kaminski H, Fissan H, Monz C, Dahmann D, Mülhopt S, Paur HR, Kiesling HJ, Herrmann F, Voetz M, Kuhlbusch TAJ (2009) Comparison of four mobility particle sizers with different time resolution for stationary exposure measurements. J Nanopart Res 11:1593–1609
27. Kaminski H, Kuhlbusch TAJ, Rath S, Götz U, Sprenger M, Wels D, Polloczek J, Bachmann V, Kiesling H-J, Dziurowitz N, Schwiegelshohn A, Monz C, Dahmann D, Asbach C (2013) Comparability of mobility particle sizers and diffusion chargers. J Aerosol Sci 57:156–178
28. Cunningham, E. (1910) On the velocity of steady fall of spherical particles through fluid medium. Proc R Soc Ser A 83:357–365
29. Kim JH, Mulholland GW, Kuckuck SR, Pui DYH (2005) Slip correction measurements of certified PSL nanoparticles using a nanometer differential mobility analyzer (Nano-DMA) for Knudsen Number from 0.5 to 83. J Res Natl Inst Stand Technol 110:31–54
30. Winkelmayr W, Reischl GP, Lindner AO, Berner A (1991) A new electromobility spectrometer for the measurement of aerosol size distributions in the size range from 1 to 1000 nm. J Aerosol Sci 22:289–296
31. Chen DR, Oui DYH, Hummes D, Fissan H, Quant FR, Sem GJ (1998) Design and evaluation of a nanometer aerosol differential mobility analyzer (Nano-DMA). J Aerosol Sci 29:497–509

32. Reischl GP, Mäkelä JM, Necid J (1997) Performance of Vienna type differential mobility analyzer at 1.2–20 nanometer. Aerosol Sci Technol 27:651–672
33. Hoppel WA (1978) Determination of the aerosol size distribution from the mobility distribution of the charged fraction of aerosols. J Aerosol Sci 9:41–54
34. Reineking A, Porstendörfer J (1986) Measurements of particle loss functions in a differential mobility analyzer (TSI, model 3071) for different flow rates. Aerosol Sci Technol 5:483–486
35. Stolzenburg MR (1988) An ultrafine aerosol size distribution measuring system, Ph.D. Thesis at the University of Minnesota
36. Wiedensohler A, Orsini D, Covert DS, Coffmann D, Cantrell W, Havlicek M, Brechtel FJ, Russell LM, Weber RJ, Gras J, Hudson JG, Litchy M (1997) Intercomparison study of the size-dependent counting efficiency of 26 condensation particle counters. Aerosol Sci Technol 27:224–242
37. Hermann H, Wehner B, Bischof O, Han H-S, Krinke T, Liu W, Zerrath A, Wiedensohler A (2007) Particle counting efficiencies of new TSI condensation particle counters. J Aerosol Sci 38:674–682
38. Shimada M, Han BW, Okuyama K, Otani Y (2002) Bipolar charging of aerosol nanoparticles by a soft X-ray photoionizer. J Chem Eng Jpn 35:786–793
39. Han BW, Shimada M, Okuyama K, Choi M (2003) Classification of monodisperse aerosol particles using an adjustable soft X-ray charger. Powder Technol 135:336–344
40. Lee HM, Kim CS, Shimada M, Okuyama K (2005) Bipolar diffusion charging for aerosol nanoparticle measurement using a soft X-ray charger. J Aerosol Sci 36:813–829
41. Levin M, Gudmundsson A, Pagels JH, Fierz M, Molhave K, Jensen KA, Koponen IK (2015) Limitations in the use of unipolar charging for electrical mobility sizing instruments. Aerosol Sci Technol 49:556–565
42. Hinds WC (1999) Aerosol technology: properties, behavior, and measurements of airborne particles, 2nd edn. Wiley, New York
43. Keskinen J, Pietarinen K, Lehtimäki M (1992) Electrical low pressure impactor. J Aerosol Sci 23:353–360
44. Watson JG, Chow JC, Chen LWA (2005) Summary of organic and elemental carbon/black carbon analysis methods and intercomparison. Aerosol Air Qual Res 5:65–102
45. Janssen NAH, Yang A, Strak M, Steenhof M, Hellack B, Gerlots-Nijland ME, Kuhlbusch T, Kelly F, Harrison R, Brunekreef B, Hoek G, Cassee F (2014) Oxidative potential of particulate matter collected at sites with different source characteristics. Sci Total Environ 472:572–581
46. Chen S-C, Wang J, Fissan H, Pui DYH (2013) Exposure assessment of nanosized engineered agglomerates and aggregates using Nuclepore filters. J Nanopart Res 15:1955
47. Dixkens J, Fissan H (1999) Development of an electrostatic precipitator for off-line particle analysis. Aerosol Sci Technol 30:438–453
48. John AC, Kuhlbusch TAJ, Fissan H (2001) Size-fractionated sampling and chemical analysis by total-reflection X-ray fluorescence spectrometry of PMx in ambient air and emissions. Spectrochim Acta Part B 56:2137–2146
49. Asbach C, Kaminski H, von Barany D, Kuhlbusch TAJ, Monz C, Dziurowitz N, Pelzer J, Vossen K, Berlin K, Dietrich S, Götz U, Kiesling H-J, Schierl R, Dahmann D (2012) Comparability of portable nanoparticle exposure monitors. Ann Occupat Hyg 56:606–621
50. Möhlmann C, Monz C, Neumann V, Dahmann D, Asbach C, Kaminski H, Todea AM (2015) From comparison tests to recommendations in standardisation for counting nanoparticles by using CPCs. Presentation at the international congress on safety of engineered nanoparticles and nanotechnologies, 12–15 April 2015, Helsinki, Finland
51. Fierz M, Houle C, Steigmeier P, Burtscher H (2011) Design, calibration, and field performance of a miniature diffusion size classifier. Aerosol Sci Technol 45:1–10
52. Marra J, Voetz M, Kiesling H-J (2009) Monitor for detecting and assesing exposure to airborne nanoparticles. J Nanopart Res 12:21–37
53. Marra J (2011) Using the Aerasense NanoTracer for simultaneously obtaining several ultrafine particle exposure metrics. J Phys Conf Ser 304:012010

54. Zhang SH, Akutsu Y, Russell LM, Flagan RC, Seinfeld JH (1995) Radial differential mobility analyzer. Aerosol Sci Technol 23:357–372
55. Tritscher T, Beeston M, Zerrath AF, Elzey S, Krinke TJ, Filimundi E, Bischof OF (2012) NanoScan SMPS: a novel, portable nanoparticle sizing and counting instrument. J Phy Conf Ser 429:012061
56. Fonseca AS, Viana M, Querol X, Todea AM, Monz C, Asbach C (2015) Intercomparison of portable (nanoScan) and stationary mobility particle sizers for nanoscale aerosol measurements. In preparation
57. Stabile L, Cauda E, Marini S, Buonanno G (2014) Metrological assessment of a portable analyzer for monitoring the particle size distribution of ultrafine particles. Ann Occup Hyg 58:860–876
58. Steer B, Gorbunov B, Muir R, Ghimire A, Rowles J (2014) Portable planar DMA: development and tests. Aerosol Sci Technol 48:251–260
59. Miller A, Frey G, King G, Sunderman C (2010) A handheld electrostatic precipitator for sampling airborne particles and nanoparticles. Aerosol Sci Technol 44:417–427
60. Fierz M, Meier D, Steigmeier P, Burtscher H (2014) Aerosol measurement by induced currents. Aerosol Sci Technol 48:350–357
61. Leith D, Miller-Lionberg D, Casuccio G, Lersch T, Lentz H, Marchese A, Volckens J (2014) Development of a transfer function for a personal, thermophoretic nanoparticle sampler. Aerosol Sci Technol 48:81–89
62. Thayer D, Koehler KA, Marchese A, Volckens J (2011) A personal, thermophoretic sampler for airborne nanoparticles. Aerosol Sci Technol 45:744–750
63. Azong-Wara N, Asbach C, Stahlmecke B, Fissan H, Kaminski H, Plitzko S, Kuhlbusch TAJ (2009) Optimisation of a thermophoretic personal sampler for nanoparticle exposure studies. J Nanopart Res 11:1611–1624
64. Azong-Wara N, Asbach C, Stahlmecke B, Fissan H, Kaminski H, Plitzko S, Bathen D, Kuhlbusch TAJ (2013) Design and experimental evaluation of a new nanoparticle thermophoretic personal sampler. J Nanopart Res 15:1530
65. Faure B, Dozol H, Brouard C, Guiot A, Clavaguera S (2015) Evaluation of a personal sampler for the assessment of mass-based exposure to airborne nanoparticles. Environ Sci Technol, Submitted
66. Cena LG, Anthony TR, Peters TM (2011) A personal nanoparticle respiratory deposition (NRD) sampler. Environ Sci Technol 45:6483–6490
67. Thongyen T, Hata M, Toriba A, Ikeda T, Koyama H, Otani Y, Furuuchi M (2015) Development of a PM0.1 personal sampler for evaluation of personal exposure to aerosol nanoparticles. Aerosol Air Qual Res 15:180–187
68. Tsai C-J, Liu C-N, Hung S-M, Chen S-C, Uang S-N, Cheng Y-S, Zhou Y (2012) Novel active personal nanoparticle sampler for the exposure assessment of nanoparticles in workplaces. Environ Sci Technol 46:4546–4552
69. Young L-H, Lin Y-H, Lin T-H, Tsai P-J, Wang Y-F, Hung S-M, Tsai C-J, Chen C-W (2013) Field application of a newly developed personal nanoparticle sampler to selected metalworking operations. Aerosol Air Qual Res 13:849–861

http://www.springer.com/978-3-319-23918-7

Indoor and Outdoor Nanoparticles
Determinants of Release and Exposure Scenarios
Viana, M. (Ed.)
2016, XVI, 236 p. 62 illus., 42 illus. in color., Hardcover
ISBN: 978-3-319-23918-7